DOI: 10.1002/chem.200500134

Laser Flash Photolysis Generation and Kinetic Studies of Corrole–Manganese(v)-Oxo Intermediates

Rui Zhang, Dilusha N. Harischandra, and Martin Newcomb*[a]

Abstract: Corrole–manganese(v)-oxo intermediates were produced by laser flash photolysis of the corresponding corrole-manganese(IV) chlorate complexes, and the kinetics of their decay reactions in CH_2Cl_2 and their reactions with organic reductants were studied. The corrole ligands studied were 5,10,15-tris(pentafluorophenyl)corrole (H_3TPFC), 5,10,15-triphenylcorrole (H_3TPC), and 5,15-bis(pentafluorophenyl)-10-(*p*-methoxyphenyl)corrole (H_3BPFMC). In self-decay reactions and in reactions with substrates, the order of reactivity of (Cor)Mn^V(O) was TPC > BPFMC > TPFC, which is inverted from that expected based on the electron-demand of the ligands. The rates of reactions of (Cor)Mn^V(O) were dependent on the concentration of the oxidant and other manganese species, with increasing concentrations of various manganese species resulting in decreasing rates of reactions, and the apparent rate constant for reaction of (TPFC)Mn^V(O) with triphenylamine was found to display fractional order with respect to the manganese-oxo species. The kinetic results are consistent in part with a reaction model involving disproportionation of (Cor)Mn^V(O) to give (Cor)Mn^{IV} and (Cor)Mn^{VI}(O) species, the latter of which is the active oxidant. Alternatively, the results are consistent with oxidation by (Cor)Mn^V(O) which is reversibly sequestered in non-reactive complexes by various manganese species.

Keywords: corroles · kinetics · laser flash photolysis · manganese

Introduction

Organic ligand-complexed transition metal-oxo intermediates are active oxidants in a variety of metal-catalyzed reactions that employ sacrificial oxidants such as hydrogen peroxide, peroxy acids, and iodosobenzene. Much research has focused on 20-membered ring macrocyclic porphyrin–metal complexes, which are mimics of heme-containing enzymes found in nature.[1] Metal complexes with corrole ligands, tetrapyrrole 19-membered macrocycles that are unsaturated analogues of the corrin ligand in cobalt-containing coenzymes, are relatively little studied.[2] Corrole–metal-oxo species are inherently more stable than the corresponding porphyrin–metal-oxo species because corroles are tri-anionic ligands, whereas porphyrins are di-anionic ligands.

Progress in methods for corrole syntheses[3] resulted in increased interest in corrole–metal complexes in recent years.[4] Catalytic oxidations with the manganese(III) complex of tris(pentafluorophenyl)corrole (H_3TPFC) using iodosobenzene as the sacrificial oxidant were reported in 2000,[5] and a biomimetic oxidation with an albumin-conjugated manganese corrole was recently reported.[6] Perhalogenation of the corrole macrocycle with bromine or fluorine results in increased reactivity as judged by turnover numbers and bulk oxidation velocities for the corrole–manganese complexes under catalytic conditions with PhIO as the sacrificial oxidant.[7,8] No kinetic information has been reported for corrole–manganese-oxo reactions, however, and the mechanisms are not well understood. For example, oxidation of the (TPFC)Mn^{III} complex with ozone gives the (TPFC)Mn^V(O) species, which does not react with styrene at room temperature,[5] an observation that led Gross and co-workers to the conclusion that the active oxidant in the catalytic process has the metal ion in a higher oxidation state than manganese(v).[5] Moreover, a high-electron demand triazacorrolazine ligand, which one might expect to give a quite reactive oxo species, in fact gives a manganese(v)-oxo complex that is stable enough to isolate.[9]

[a] R. Zhang, D. N. Harischandra, Prof. M. Newcomb
Department of Chemistry
University of Illinois at Chicago
845 W. Taylor St., Chicago, IL 60607 (USA)
Fax: (+1) 312-996-0431
E-mail: men@uic.edu

Supporting information for this article is available on the WWW under http://www.chemeurj.org/ or from the author: Spectra of (Cor)Mn^V(O), spectrum from reaction of **4a** with *cis*-cyclooctene, results of laser power studies, and spectrum from reaction of **4a** with **1a**.

We recently introduced the use of laser flash photolysis (LFP) methods for formation and kinetic studies of porphyrin–manganese-oxo derivatives[10,11] and for photo-oxidations that give compound I and analogues, iron(IV)-oxo porphyrin radical cations.[12] With photochemical production of reactive metal-oxo transients, one has access to time scales that are much shorter than the fastest mixing experiments, and kinetics of oxidation reactions of the transients of interest are not convoluted with the kinetics of reactions that form the transients. In the present work, we report photolysis reactions of triarylcorrole–manganese(IV) chlorate complexes that result in homolytic cleavage of the O–Cl bond in the chlorate to give triarylcorrole–manganese(V)-oxo species and kinetic studies of (Cor)Mn^{V}(O) species formed under various conditions. The kinetic results demonstrate that reactions of (Cor)Mn^{V}(O) are mechanistically complex, and, in part, they are consistent with the premise that the predominant oxidants in these systems are corrole–manganese(VI)-oxo species formed at concentrations too small for detection.[5] We also observed corrole–manganese concentration-dependent inhibition of the oxidation reactions and fractional kinetic order with respect to (Cor)Mn^{V}(O), however, which suggests an alternative mechanistic Scheme where the corrole–manganese(V)-oxo species are the active oxidants but can be sequestered in unreactive complexes.

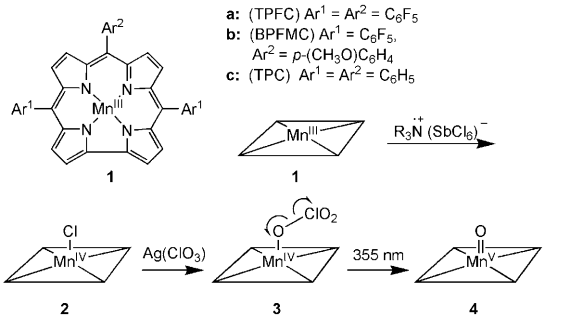

Scheme 1.

Results

We studied the three triarylcorrole–manganese systems shown in Scheme 1. Using abbreviations that follow those established by Gross, the 5,10,15-tris(pentafluorophenyl)corrole system, labeled "**a**" in this work, is (H_3TPFC), and the 5,10,15-triphenylcorrole system labeled "**c**" is (H_3TPC). The 5,15-bis(pentafluorophenyl)-10-(*p*-methoxyphenyl)corrole system (**b**) is abbreviated (H_3BPFMC). Each of the corrole ligands was known,[3,13,14] as were the manganese(III) complexes **1a**[5] and **1c**,[15] but the manganese derivative **1b** is new.

Oxidation of the neutral triarylcorrole–manganese(III) species **1** with tris(4-bromophenyl)aminium hexachloroantimonate gave the corrole–manganese(IV) chloride salts **2**, **2a**[7] and **2c**[15] were known. The by-product of the oxidation reaction, Ar_3N, would interfere with kinetic studies, and complexes **2** were purified by crystallization followed by repeated silica gel chromatographies until no amine could be detected in the UV-visible spectrum. We note that silica gel chromatography of corrole–manganese(IV) chlorides has not been reported previously, but UV-visible spectra and thin layer chromatography showed that the method does not result in exchange of the tightly bound chloride anion; it is well known that porphyrin–metal(III) chloride complexes can be successfully purified by silica gel chromatography.[16] Exchange of the counterion in **2** with Ag(ClO_3) gave the corresponding chlorate salts **3** that were the desired photochemical precursors. Chlorate salts **3** were prepared in situ and used in LFP studies immediately after preparation; they were identified only by their UV-visible spectra. The UV-visible spectra of the various corrole species **1**, **2**, and **3** are listed in Table 1. The neutral corrole complexes **1** and chloride salts **2** displayed split Soret bands, but the chlorate salts **3** did not, as illustrated in Figure 1 for the (TPFC) salts.

Table 1. UV-visible absorbances for corrole manganese complexes.[a]

Complex	Soret bands (log ε)	Q bands (log ε)
(TPFC)Mn^{III} (**1a**)	399 (4.59), 416 (4.62)	484 (4.30), 596 (4.04)
(BPFMC)Mn^{III} (**1b**)	399 (4.29), 419 (4.26)	488 (4.10), 583 (3.72), 631 (3.76)
(TPC)Mn^{III} (**1c**)	403 (4.42), 438 (4.30)	500 (3.86), 651 (3.55)
(TPFC)Mn^{IV}(Cl) (**2a**)	363 (4.42), 415 (4.67)	589 (3.63)
(BPFMC)Mn^{IV}(Cl) (**2b**)	360 (4.15), 411 (4.32)	600 (4.17)
(TPC)Mn^{IV}(Cl) (**2c**)	358 (4.49), 433 (4.66)	603 (3.61)
(TPFC)Mn^{IV}(ClO_3) (**3a**)	429 (4.70)	595 (3.79)
(BPFMC)Mn^{IV}(ClO_3) (**3b**)	421 (4.36)	592 (3.57)
(TPC)Mn^{IV}(ClO_3) (**3c**)	439 (4.67)	611 (3.45)

[a] Spectra in CH_2Cl_2 solutions.

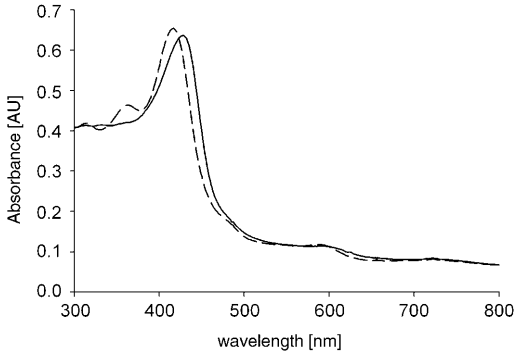

Figure 1. UV/Vis spectra of (TPFC)Mn^{IV}Cl (**2a**) (dashed line) and (TPFPC)Mn^{IV}(ClO_3) (**3a**) (solid line).

Irradiation of chlorate complexes **3** with 355 nm light from a Nd/YAG laser gave results shown in Figures 2 and 3. In Figure 2, we show the spectrum produced by LFP of pre-

cursor **3a**; the Soret band from **3a** was bleached, and new signals were produced that were blue-shifted. Addition of a scaled spectrum of the bleached precursor to the LFP spectrum gave the product spectrum of (TPFC)Mn^{V}(O) (**4a**), which is the same as the spectrum of **4a** formed by chemical oxidation of the neutral corrole–manganese(III) species **1a** (Figure 2b). The spectrum of photogenerated **4a** also matched that reported previously from ozone oxidation of the species **1a**.[5] In Figure 3, we show spectra of **4b** and **4c** formed by LFP of the corresponding chlorate salts, which match the UV/vis spectra obtained by chemical oxidation of the respective (Cor)Mn^{III} species **1b** and **1c** (Supporting Information).

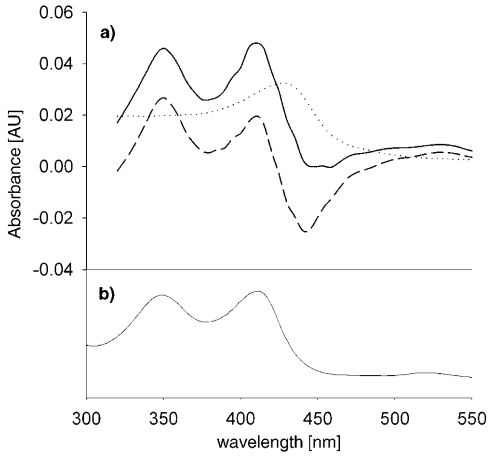

Figure 2. a) LFP spectrum observed upon irradiation of (TPFC)Mn^{IV}-(ClO_3) in CH_2Cl_2 (**3a**) (dashed line), spectrum of chlorate salt **3a** scaled to give zero absorbance at 450 nm (dotted line), and spectrum of **4a** from addition of the two spectra (solid line). b) Spectrum of (TPFC)Mn^{V}(O) (**4a**) formed by reaction of the neutral complex **1a** with PhIO.

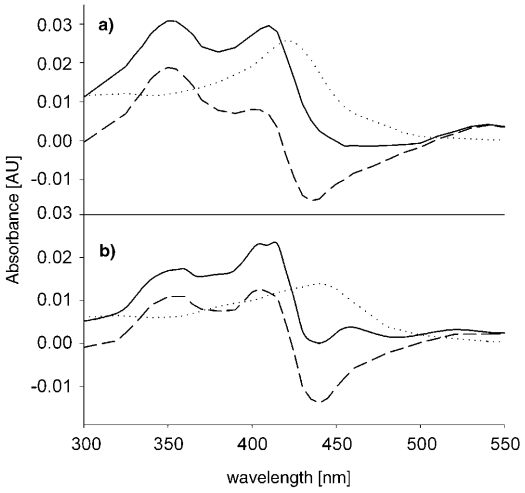

Figure 3. a) Spectrum of (BPFMC)Mn^{V}(O) (**4b**). b) Spectrum of (TPC)Mn^{V}(O) (**4c**). The dashed lines are the LFP results, the dotted lines are scaled spectra of the precursors **3**, and the solid lines are spectra of derivatives **4** obtained by addition of the other two spectra.

Table 2. Spectra of corrole–manganese(v)-oxo derivatives **4** formed by LFP.[a]

(Cor)Mn^{V}(O)	Absorption bands[b] (log ε)[c]	Quantum yield[d]
(TPFC)Mn^{V}(O) (**4a**)	350 (4.62), 410 (4.65), 525 (4.01)	1.6×10^{-2}
(BPFMC)Mn^{V}(O) (**4b**)	354 (4.34), 410 (4.36), 535 (3.76)	1.7×10^{-2}
(TPC)Mn^{V}(O) (**4c**)	356 (4.34), 415 (4.47), 550 (3.77)	3.2×10^{-2}

[a] In CH_2Cl_2 solutions. [b] Absorption bands in nm. [c] The molar extinction coefficients were determined with samples of **4** prepared by oxidation of **1** with PhIO. [d] From photolysis of precursors **3**, in units of mol/einstein of 355 nm light.

The UV/Vis spectra of oxo species **4** have split Soret bands that are distinct and considerably blue-shifted from the Soret band of the chlorate complexes **3** (Table 2). Thus, the photolysis reactions of the chlorate complexes **3** produced neutral oxo-species **4** by homolytic cleavage of the O–Cl bond in the chlorate counterion. The photo-induced fragmentation reactions of chlorates **3** are directly analogous to the photochemical cleavages of porphyrin–manganese(III) chlorates, which give neutral porphyrin-manganese(IV)-oxo derivatives by homolytic cleavage of the O–Cl bonds in the chlorates.[11]

The photochemical reaction giving **4a** in CH_2Cl_2 was shown to be a one-photon process in variable power experiments. Specifically, the slope of a plot of the logarithm for formation of **4a**, as determined by signal intensity at 350 nm, versus the logarithm of laser power from 24 to 85 mJ was 1.14 ± 0.24 (error at 2σ) (Supporting Information). The quantum yields for formation of oxo complexes **4** are given in Table 2. These values were determined with benzophenone as the actinometric standard, where the quantum efficiency for formation of the benzophenone triplet with 355 nm light is taken to be 100 %.[17] The photo-induced cleavages of the chlorate salts **3** are reasonably efficient processes, and they would result in about 10 % conversion if 40 mJ of 355 nm light was used. The quantum yields for reactions of **3** are similar to those found for photo-induced homolytic cleavages of the O–Cl bonds in porphyrin–manganese(III) chlorate complexes.[11]

The photochemically-generated corrole–manganese(v)-oxo species **4** in CH_2Cl_2 solutions decayed, initially giving corrole–manganese(IV) species. In the example in Figure 4, one of the split Soret bands of **4a** overlaps with the major Soret band of chloride salt **2a** and the single Soret band of chlorate salt **3a**, with the result that the decrease in absorbance at 400 nm over the course of the decay reaction is somewhat less than the decay observed at 350 nm. The formation of manganese(IV) species in these reactions does not implicate one-electron reactions because the decay reactions are relatively slow. Reaction of oxo species **4** in two-electron reactions to give **1** followed by comproportionation of **1** with another molecule of **4** is possible, and the reaction of **1a** with **4a** was demonstrated (Supporting Information).

The decay reactions of species **4** were complex. The half-lives of **4** when they were produced at about 5×10^{-7} M con-

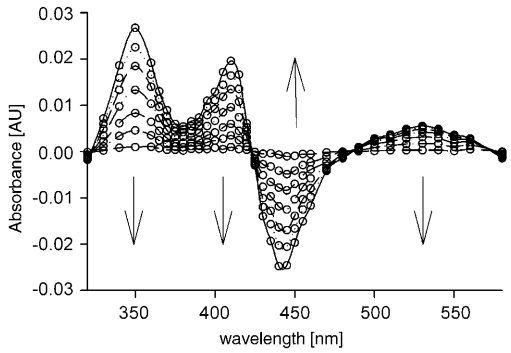

Figure 4. Decay spectrum for species **4a** reacting in CH_2Cl_2 solution over 10 s. In this representation, decaying signals show as positive absorbances, and growing signals show as negative absorbances.

centration at ambient temperature in CH_2Cl_2 were in the range of 1–10 seconds, but the rates of decay were dependent on the concentrations of manganese species. Table 3

Table 3. Manganese species concentration effects on decay of corrole–manganese(v)-oxo species **4**.[a]

Oxo species[b] (M conc)	Additive (M conc)	k_{obs} [s^{-1}][b]
4c (6×10^{-7})	**3c** (2×10^{-5})	1.5
4b (5×10^{-7})	**3b** (2×10^{-5})	0.14
4a (0.6×10^{-7})	**3a** (0.25×10^{-5})	0.26
4a (1.2×10^{-7})	**3a** (0.5×10^{-5})	0.23
4a (2.5×10^{-7})	**3a** (1×10^{-5})	0.16
4a (5×10^{-7})	**3a** (2×10^{-5})	0.10
4a[c] (1.6×10^{-5})	none	1.6×10^{-3}
4a[c] (2.9×10^{-5})	none	5.4×10^{-4}
4a[c] (1.6×10^{-5})	**3a** (1.8×10^{-5})	5.2×10^{-5}
4a[c] (1.6×10^{-5})	**2a** (1.8×10^{-5})	8.1×10^{-4}

[a] Observed first-order decay rate constants in CH_2Cl_2 at 20 ± 2°C. [b] Oxo species **4** produced in LFP experiments unless noted. [c] Oxo species produced by MCPBA oxidation of **1a**.

lists apparent pseudo-first-order rate constants for decay of **4**. We note that we solved the kinetic data for first-order decay in order to illustrate concentration effects, but the reactions are not cleanly first-order in oxidant. When the concentrations of species **4a** increased, the apparent rate of decay *decreased*. From the LFP studies, one cannot determine if the kinetic inhibition was due to oxo species **4a** or its precursor **3a** (or both) because the concentrations of **4a** and precursor **3a** changed linearly, but stopped-flow studies with **4a** formed by stoichiometric oxidation of precursor **1a** by *m*-chloroperoxybenzoic acid (MCPBA) showed that any manganese species tested had a suppressing effect on the rates of decay. Thus, an increase in concentration of **4a** in the absence of other manganese species resulted in a decrease in the rate of decay. Addition of manganese(IV) salts **2a** and **3a** also reduced the rate of decay of **4a**; the difference in effects of the two manganese(IV) salts likely reflects differences in the strengths of the axial ligand bonds. We note that, in the extreme examples in Table 3, the apparent rate constants for decay of oxo species **4a** differed by nearly four orders of magnitude, and extrapolation of the results to high concentrations of manganese species would lead to the conclusion that concentrated **4a** should appear to be relatively stable. As discussed later, this concentration-dependent kinetic suppression effect likely was an important factor in the paradoxical reactivity behavior previously reported for (TPFC)Mn^{V}(O).[5,7,8,18]

Reactions of oxo species **4** in CH_2Cl_2 with alkenes, Ph_3P, and Ph_3N were studied. The amounts of transients **4** produced in LFP studies were in the range of 10–50 pmol; therefore, products could be characterized spectroscopically but not isolated. Previous studies led to conflicting reports that (TPFC)Mn^{V}(O) (**4a**) either does[8] or does not[5] react with alkenes, but we observed reactions of transients **4** with alkenes. Corrole–manganese complex **1a** is known to catalyze oxidation of alkenes to the expected epoxide products under turnover conditions with PhIO as the sacrificial oxidant,[5,8] and we confirmed these results in studies with *cis*-cyclooctene and *cis*-stilbene (see below). Triphenylphosphine is known to be oxidized to $Ph_3P(O)$ by **4a** produced under any conditions.[5] We also studied reactions of species **4** with Ph_3N, which typically reacts with metal-oxo species by one-electron transfer; the triphenylamminium radical cation was observed spectroscopically (λ_{max} ≈650 nm) in our studies, confirming that one-electron reduction of **4** occurred at least in part.

As expected from the decay reactions in the absence of substrates, reactions of **4** with substrates displayed complex kinetics. Nonetheless, apparent pseudo-first-order decay rate constants for **4** increased linearly as a function of substrate concentration (Figure 5), thus permitting calculation of ap-

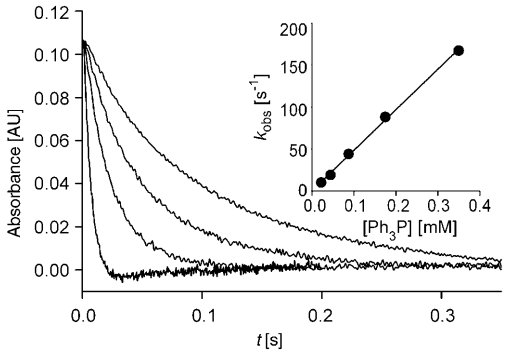

Figure 5. Kinetic decay traces at 350 nm for reaction of 5×10^{-7} M **4a** in the presence of (from the top) 0.044, 0.088, 0.18, and 0.35 mM Ph_3P. The inset shows observed pseudo-first-order decay rate constants as a function of substrate concentration.

parent second-order rate constants for reactions with the reductants via Equation (1) where k_{obs} is the observed pseudo-first-order rate constant, k_0 is a background decay rate constant, k_{ox} is the apparent second-order rate constant for reaction with substrate, and [Sub] is the concentration of substrate. Apparent second-order rate constants for reactions with the various substrates are listed in Table 4, where we

Table 4. Rate constants for reactions of corrole–manganese(v)-oxo species **4**.[a]

Oxo species	Substrate	k_{ox} [$M^{-1}s^{-1}$]
4a	Ph_3N	$(1.35 \pm 0.1) \times 10^4$
	Ph_3P	$(4.9 \pm 0.2) \times 10^5$
	cyclohexene	16 ± 2
	cyclooctene[b]	4 ± 1
	cis-stilbene	9 ± 2
4b	Ph_3N	$(3.0 \pm 0.6) \times 10^4$
	Ph_3P	$(7.2 \pm 0.4) \times 10^5$
4c	Ph_3N	$(5.2 \pm 0.4) \times 10^4$
	Ph_3P	$(8.0 \pm 0.4) \times 10^5$
	cyclohexene	33 ± 5
	cyclooctene[b]	11 ± 2
	cis-stilbene	20 ± 2
	styrene	< 1

[a] Apparent second-order rate constants for reactions of 5×10^{-7} M **4** at 20 ± 2 °C in CH_2Cl_2 solutions. [b] *cis*-cyclooctene.

used the same initial concentration of each oxo species **4** for all reactions.

$$k_{obs} = k_0 + k_{ox}[Sub] \quad (1)$$

Manganese concentration effects for reactions of **4** with substrates mirrored those found for decay in the absence of reactive substrate. In a series of LFP experiments, we produced varying concentrations of **4a** by changing the concentrations of precursor **3a**, and measured apparent pseudo-first-order rate constants for reaction of **4a** in the presence of 0.8 mM Ph_3N. The observed rate constants decreased as the concentration of **4a** increased (Figure 6). When the data was plotted in log–log format (inset in Figure 6), the slope

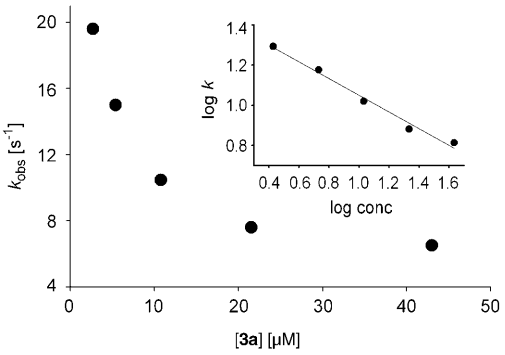

Figure 6. Observed apparent pseudo-first-order rate constants for reaction of **4a** in CH_2Cl_2 in the presence of 0.8 mM Ph_3N. The concentrations of precursor **3a** are listed; under the LFP conditions used, the conversions of **3a** to **4a** were ca. 2.5% efficient. The inset shows the data in log-log format.

was about −0.4, where a slope of −0.5 would be found for a reaction that is one-half order in **4a**. The experimental data cannot be fit precisely for half-order reactions of **4a**, but the results indicate that the kinetic order for **4a** is less than one. This behavior implicates one or more kinetically important aggregation phenomena.

A dramatic suppression of the rate of reaction of oxo species **4a** with *cis*-cyclooctene as a function of increased **4a** concentration was demonstrated. In a series of stopped-flow mixing studies, **4a** at a concentration of 2×10^{-5} M was produced by MCPBA oxidation of **1a** and allowed to react with *cis*-cyclooctene at concentrations ranging from 0.1 to 1.4 M (Supporting Information). The complexity of the reactions was indicated in the time-resolved spectra that did not contain isosbestic points, but it is noteworthy that the only detectable manganese product was (TPFC)Mn^{III} (see Figure S2 in Supporting Information). Analysis of the data via Equation (1) gave an apparent second-order rate constant of $k_{ox} = 0.12 \pm 0.02\,M^{-1}s^{-1}$, which can be compared with the value obtained for more dilute **4a** given in Table 4. Thus, a about 40-fold *increase* in concentration of **4a** resulted in a 33-fold *decrease* in the apparent second-order rate constant.

Despite the complications of concentration effects, two trends appear to be important in Table 4, where the initial concentrations of species **4** were constant in all studies. For any given reductant, the reactivities of oxo species **4** are inverted with the more electron-demanding ligand (TPFC) giving the least reactive oxo species **4a** and the least electron-demanding ligand (TPC) giving the most reactive oxo species **4c**. The second feature is subtle. In the two-electron oxo-transfer reactions, oxidations of the alkenes and reactions with Ph_3P, the difference in the apparent second-order rate constants for species **4a** and **4c** are effectively constant even through the absolute reactivities of Ph_3P with oxo species **4** are 4–5 orders of magnitude greater than the reactivities of the alkenes. Mechanistic models with different reactive oxidants are possible, as discussed later, but these results suggest that only one *active* oxidant was involved in the LFP reactions.

Collman and co-workers reported evidence that corrole–manganese species **1a** can effect oxidations via a complex of the sacrificial oxidant PhIO with manganese as well as by reaction of the metal-oxo species **4a**.[18] We briefly evaluated that model by conducting competitive oxidation reactions with *cis*-cyclooctene and *cis*-stilbene. Thus, mixtures of the two alkenes and a catalytic amount of **1a** or **1c** in CH_2Cl_2 were treated with a limited amount of PhIO, the reactions were allowed to proceed essentially to complete consumption of the PhIO, and the amounts of epoxides formed in the reactions were determined by GC and ^1H NMR measurements. The relative rates of oxidation of the substrates under catalytic turnover conditions differed considerably from the ratios of rate constants found in the LFP studies. The ratio of LFP rate constants for reactions of **4a** with cyclooctene and with stilbene was 0.4, but cyclooctene was oxidized 1.4 times faster than stilbene in the catalytic turnover reactions. Similarly, the LFP rate constant ratio for reaction of **4c** with cyclooctene and stilbene was 0.5, whereas the product ratio from the two alkenes under catalytic turnover conditions was 1.5. The complex concentration effects on kinetics preclude a simple explanation, but the active oxidants under catalytic turnover conditions with PhIO appear not to be the same as those produced by photochemical generation of (Cor)Mn^V(O).

Discussion

Photochemical activation of transition metal complexes to produce reactive oxidants has been known for years,[19] but the use of laser flash photolysis (LFP) methods to produce and study reactions of manganese-oxo transients in real time was introduced only recently.[10,11] From a mechanistic perspective, direct kinetic studies of transition metal-oxo derivatives offer some advantages over product and turnover studies. The kinetics of oxidation reactions by the metal-oxo species can be determined under pseudo-first-order reaction conditions with respect to the reductant, thus providing precise rate constants, and the kinetics of oxidations by photogenerated metal-oxo species are not convoluted with the rate constants for formation of the reactive transients by reaction of the sacrificial oxidant with the low-valent metal species.

Despite the precision of the LFP method, the rate constants for reactions of transients **4** obtained in this work are not true second-order rate constants for reactions of **4**. The concentration-dependent behavior of the rate constants indicates that equilibration reactions were important in the kinetics, and one cannot determine with certainty what species are the active oxidants. For example, oxo-species **4a** produced by ozone oxidation of **1a** appeared to be a relatively stable compound in CH_2Cl_2 that did not react with styrene,[5] but **4a** appears to be highly reactive with alkenes in CH_2Cl_2 when formed photochemically in this work, and alkene epoxidation reactions with catalytic **1a** and PhIO as the sacrificial oxidant are facile.[5,7,8,18]

The stability of **4a** produced by ozone oxidation of **1a** led Gross and co-workers to conclude that **4a** was not the active oxidant for styrene and that a higher valence manganese species was active under catalytic turnover conditions.[5] A model for production and reaction of such species is shown in Figure 7. Two-electron oxidation of neutral corrole–manganese(III) species **1** by PhIO will give the corrole–manganese(v)-oxo derivative **4**, and two molecules of **4** could react in a disproportionation reaction to give (Cor)Mn^{VI}(O)(X) and (Cor)Mn^{IV}(X). It also is possible that **4** will react with **1** in a comproportionation process that gives two manganese(IV) species, and we observed that a mixture of **4a** and **1a** reacted slowly to give manganese(IV) species. (Cor)Mn^{IV} species are cations that might be viewed as analogues of cationic (porphyrin)Mn^{III} species, which are oxidized by sacrificial two-electron oxidants to cationic (porphyrin)Mn^{V}(O) species.[10,11,20–22] Therefore, PhIO oxidation of cationic (Cor)Mn^{IV} to cationic (Cor)Mn^{VI}(O) might be expected, and the manganese(VI)-oxo species could be the active oxidant. Importantly, the recent report of characterization of a corrole–manganese(VI)-nitrido species shows that such high oxidation state manganese species are accessible.[23] In the model in Figure 7, the oxidizing system could shuttle between (Cor)Mn^{IV} and (Cor)Mn^{VI}(O) cations after the initial oxidation of the (Cor)Mn^{III} complex. In the LFP studies, where sacrificial oxidants are not present, the velocities of reactions would reflect the populations of (Cor)Mn^{VI}(O) cations that are determined by the disproportionation equilibrium constant. In either case, the concentration of the active oxidant could be too small to permit detection, and the major species observed spectroscopically might be (Cor)Mn^{V}(O).

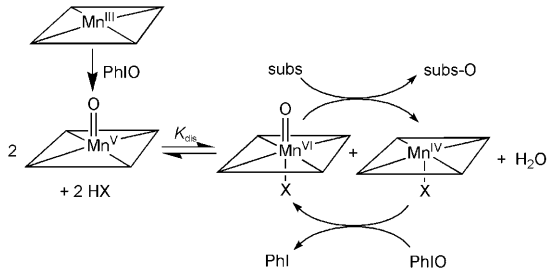

Figure 7. Model for oxidations by corrole–manganese(VI)-oxo species. The parallelograms represent corrole ligands.

The mechanistic model in Figure 7 is similar to that proposed for reactions of neutral porphyrin–manganese(IV)-oxo species, where the actual oxidants in the systems apparently are cationic porphyrin–manganese(v)-oxo species formed in disproportionation equilibria.[11] Much of the experimental results in the present work can be accommodated by this model. Perhaps the most compelling results in its support are the inverted reactivity patterns found for the corrole systems studied. In porphyrin–metal-oxo chemistry, one typically observes that more electron-withdrawing ligands give more reactive metal-oxo derivatives,[24–26] and this was specifically demonstrated for a series of porphyrin–manganese(v)-oxo complexes in reactions with a variety of substrates.[10,11] For the corrole systems studied here, the reactivity order is inverted with the system with least electron demand, the triphenylcorrole complex **4c**, apparently reacting fastest with any given substrate. If (Cor)Mn^{VI}(O) cations are the actual oxidants, then the equilibrium reactions for formation of these species should be most favorable for the ligand that has the least electron demand. Accordingly, the observed kinetics could reflect the populations of the (Cor)Mn^{VI}(O) cations, which should be largest for the TPC ligand. Our finding that added (Cor)Mn^{IV} salts suppress the rates of reactions of (Cor)Mn^{V}(O) also is consistent with the reaction model in Figure 7 because the added salts would drive the equilibrium shown in the Figure to the left.

The mechanistic model in Figure 7 does not, however, provide a good explanation for the apparent fractional kinetic order of **4**. The disproportionation equilibrium as shown would reduce the concentration of active oxidant, but reactions would still be first-order in species **4**. The mechanism also does not readily explain why **4a** produced at high concentration in the ozone oxidation of **1a** was relatively stable.[5] Another aspect of the present results does not fit this model well. If (TPFC)Mn^{V}(O) (**4a**) is produced by stoichiometric reaction of **1a** with MCPBA and then allowed to react with an alkene, the manganese product predicted by this Scheme is an unreactive (TPFC)Mn^{IV} cation. In practice, the reaction of **4a** with *cis*-cyclooctene returned neutral **1a**, and there was no evidence for accumulation of any

(TPFC)Mn^{IV} species during the reaction (Figure S2 in Supporting Information). Similar behavior was previously reported by Chang and co-workers.[8]

The findings that species **4** has fractional kinetic order and that increasing concentrations of various manganese species reduce the velocities of reactions indicate that the reactive oxo species are sequestered in inactive forms. It appears possible that the active oxidant can be bound in weak complexes that are produced without redox reactions (Figure 8). Fractional kinetic order for **4** is predicted for such complexation, and this model would predict the formation of (Cor)Mn^{III} species as the manganese products in reactions with substrates. The observed[5] stability of **4a** when produced by ozone oxidation of **1a** might reflect a concentration effect on reactivity similar to those we found in this work but more dramatic due to higher concentrations of **4a**. The inverted reactivity pattern for the corrole systems studied here also can be rationalized in the context of this model. As the electron demand is increased in the corrole ligand, the manganese ions would bear more positive charge, resulting in more tightly bound complexes and smaller concentrations of active oxidant.

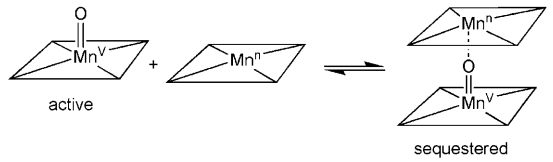

Figure 8. Oxidant sequestering model for oxidations by corrole–manganese(v)-oxo species.

The scheme for reactions of corrole–manganese-oxo species presented by Collman and co-workers also should be considered.[18] In their model, oxidations are effected by (Cor)Mn^{V}(O) species and also by complexes of the (Cor)-Mn^{III} species with the sacrificial oxidants ArIO. Goldberg and co-workers proposed a related model where catalyzed oxidations were effected by PhIO complexes with (corrolazine)Mn^{V}(O).[27] Our limited studies of competitive oxidations gave results consistent with the formation of a different or additional oxidant when PhIO was used as a sacrificial oxidant, but the model does not provide a rationalization for the kinetic results we found when no sacrificial oxidant was present. The changes in rates as a function of concentrations of various manganese species require some type of equilibria involving these species.

It is interesting to note that the effects found by Collman and co-workers, different product ratios in competitive oxidations with different ArIO sacrificial oxidants,[18] as well as those we found, product ratios in catalytic reactions with PhIO that did not match the ratios of rate constants from the LFP results, might be explained in the context of oxidations via the mechanism in Figure 7 *if* both (Cor)Mn^{VI}-(O)(X) and (Cor)Mn^{V}(O) are active oxidants. However, a "two active oxidants" model is not suggested by the observation that the reactivity ratios for **4a** and **4c** with alkenes and with Ph_3P were essentially constant.

A considerable amount of kinetic information was accumulated in this work, but the details of corrole–manganese-oxo oxidations remain elusive. Two mechanistic models, oxidations by (Cor)Mn^{VI}(O)(X) produced at low concentrations by disproportionation of (Cor)Mn^{V}(O) and oxidations by "free" (Cor)Mn^{V}(O) that equilibrates with inactive "sequestered" forms, appear to accommodate most of the results. Both models predict that an increase in the electron withdrawing effects of the corrole ligand could give manganese-oxo species that are apparently less reactive because the populations of active oxidants are smaller, thus providing a rationalization for the inverted reactivity patterns for **4** we found as well as the stability of the high-electron-demand triazacorrolazine–manganese-oxo species observed by Goldberg and co-workers.[9] In addition, multiple oxidant forms might be involved under catalytic turnover conditions, although a single oxidant form appears to be involved when the oxo species are formed photochemically, as deduced from the reactivity patterns in Table 4.

Experimental Section

Materials: Methylene chloride was obtained from Fisher Scientific and distilled over CaH_2 prior to use. Pyrrole (98%) was purchased from Sigma-Aldrich Chemical Company and distilled before use. Pentafluorobenzaldehyde and trifluoroacetic acid (TFA) (99%) were purchased from Aldrich Chemical Company and used as received. Benzaldehyde was purchased from Aldrich Chemical Company and distilled under vacuum prior to use. 2,3-Dichloro-5,6-dicyano-1,4-benzoquinone (DDQ) was obtained from Aldrich Chemical Company and used as received. Iodosobenzene was purchased from TCI America Company. *m*-Chloroperoxybenzoic acid (MCPBA) (77%) from Aldrich Chemical Company was purified by crystallization from methylene chloride and dried in vacuum. All reactive substrates for LFP kinetic studies and catalytic competitive oxidations were the best available purity (Aldrich) and were passed through a dry column of active alumina (Grade I) before use. Corrole ligands employed in this study, H_3TPFC,[3] H_3TPC,[13] and H_3BPMFC,[14] were prepared according to the literature procedures, and their characterization data (^{1}H NMR, UV/Vis and HRMS-ESI) were consistent with reported values.

Corrole–manganese(III) complexes (1): The complexes were prepared as previously described.[5] In a typical procedure, a solution of H_3TPFC (50 mg, 68 μmol) and manganese(II) acetate tetrahydrate (167 mg, 680 μmol) in DMF was heated at reflux for 30 min. Evaporation of solvent followed by column chromatography on silica gel (hexane/ethyl acetate 5:1), resulted in isolation of the desired corrole–manganese(III) complex in 90% yield. The UV/Vis spectra of compounds **1** are listed in Table 1.

(TPFC)Mn^{III} (1a):[5] FAB-MS: m/z: 848.2 $[M]^+$, 849.2 $[M+H]^+$.

(BPMFC)Mn^{III} (1b):[5] FAB-MS: m/z: 788.2 $[M]^+$, 789.2 $[M+H]^+$.

(TPC)Mn^{III} (1c):[5] FAB-MS: m/z: 578.5 $[M]^+$, 579.5 $[M+H]^+$.

Corrole–manganese(IV) chlorides (2): The compounds were prepared by a previously reported procedure.[7] In a typical preparation, a hexane solution of Mn^{III}TPFC (2.5 mg, 3.2 μmol) was treated with a dichloromethane solution of tris(4-bromophenyl)aminium hexachloroantimonate (2.6 mg, 3.2 μmol), which resulted in quantitative precipitation of Mn^{IV}TPFC(Cl). Recrystallization from CH_2Cl_2/hexane was followed by two column chromatographies on silica gel to remove traces of the amine by-product. In the purified products (90–95% yield), no amine was detected by UV/Vis at its λ_{max} value of 312 nm. The UV/Vis spectra of compounds **2** are listed in Table 1.

(TPFC)Mn^{IV}Cl (2a):[7] LRMS (ESI): m/z: 848.4 $[M-Cl]^+$.

(BPMFC)Mn^{IV}Cl (2b): LRMS (ESI): m/z: 788.2 $[M-Cl]^+$.

(TPC)Mn^{IV}Cl (2c):[15] LRMS (ESI): m/z: 578.5 $[M-Cl]^+$.

Corrole–manganese(IV) chlorates (3): The compounds were prepared in situ by stirring (Cor)Mn^{IV}Cl with excess amounts of silver chlorate ($AgClO_3$) in CH_2Cl_2 followed by filtration. The formation of chlorate products **3** was indicated by the change of UV/Vis absorption (Table 1). The resulting solutions were used for LPF studies immediately after preparation.

Instrumentation: UV/Vis spectra were recorded on an Agilent 8453 spectrophotometer. Laser flash photolysis studies were conducted on an LK-60 kinetic spectrometer (Applied Photophysics) at ambient temperature (20 ± 2 °C). Solutions of (Cor)Mn^{IV}(ClO_3) with concentrations of ca. 2×10^{-5} M (after mixing) in methylene chloride were irradiated with 355 nm light from a Nd/YAG laser (ca. 7 ns pulse). Data was acquired and analyzed with the Applied Photophysics software. Oversampling (64:1) was employed in some cases to improve the signal to noise ratios. For kinetic studies, an SC-18 mV stopped-flow mixing unit affixed to the kinetic spectrometer was employed. For generation of (Cor)Mn^{V}(O) species in mixing studies, an RX2000 rapid kinetics spectrometer accessory (Applied Photophysics) coupled with the above UV spectrometer was employed with 400 ms to seconds time scales; solutions of (Cor)Mn^{III} complexes were treated with *equivalent* amounts of MCPBA or PhIO.

Quantum yields: The values were determined relative to the yield of a standard by the general method of Hoshino.[17] A solution of the (Cor)Mn^{IV}(ClO_3) complex **3** with an absorbance of 0.5 at 355 nm was irradiated with the third harmonic of the Nd/YAG laser (355 nm) at 30 mJ of power per pulse, and the absorption at λ_{max} for the ca. 350 nm band of (Cor)Mn^{V}(O) product **4** was measured. The molar yield of **4** was determined from the extinction coefficients found in the mixing studies (Table 2). The yield of **4** was compared with the yield of benzophenone triplet formed by 355 nm irradiation of a solution with an absorbance of 0.5 at 355 nm. In this method, the quantum yield for excitation of benzophenone is taken to be 1.0.[17] The quantum yield was calculated from the ratio of molar yields and ratio of molar extinction coefficients for the product of interest and the benzophenone triplet.

Kinetics: In LFP studies, solutions of precursor **3** were irradiated by the laser, and decay of **4** at λ_{max} was monitored. For reactions with substrates, solutions of **3** were mixed with solutions of substrate at varying concentrations, the resulting mixtures were irradiated by the laser after a delay of < 1 s, and decay of (Cor)Mn^{V}(O) (**4**) was followed at λ_{max}. For stopped-flow mixing studies, **1a** in CH_2Cl_2 solution was oxidized with 1.0 equivalent of MCPBA, and the resulting solution containing **4a** was mixed with CH_2Cl_2 solutions of *cis*-cyclooctene. The kinetic results were complex but could be fit reasonably well for single exponential processes. For each reaction with substrate, four or five concentrations of substrate were studied. All kinetic runs are the average of three independent determinations. Apparent second-order rate constants for reactions of **4** with substrates were determined from the observed decay rate constants with Equation (1). All errors listed are 2σ.

Competitive oxidations: Solutions containing *cis*-stilbene (0.25 mmol), *cis*-cyclooctene (0.25 mmol) and (Cor)Mn^{III} (5 μmol) in CH_2Cl_2 were prepared. PhIO (0.125 mmol) was added, and the mixture was stirred under a nitrogen atmosphere at ca. 22 °C until the PhIO was consumed. The reaction mixture was passed through a short silica gel column and analyzed by GC after addition of an internal standard or, after concentration, by ^{1}H NMR spectroscopy of a $CDCl_3$ solution. The products were identified by comparison to authentic samples. The products from *cis*-stilbene were *cis*- and *trans*-stilbene oxide (*cis*/*trans* 5:1), quantitated using their characteristic singlets at δ 4.3 and 3.8, respectively, and a trace of benzaldehyde (<5%). For *cis*-cyclooctene, the only product detected was *cis*-cyclooctene oxide. Total yields based on PhIO were ca. 60% as determined by quantitative GC. The product ratios listed in the text (determined by GC and/or NMR integration) are the averages of three determinations.

Acknowledgements

This work was supported by a grant from the National Institutes of Health (GM 48722).

[1] B. Meunier, *Chem. Rev.* **1992**, *92*, 1411–1456. J. P. Collman, X. Zhang, V. J. Lee, E. Uffelman, J. I. Brauman, *Science* **1993**, *261*, 1404–1411; *Metalloporphyrins in Catalytic Oxidations* (Ed.: R. A. Scheldon), Marcel Dekker, New York, **1994**; *Metal-Oxo and Metal-Peroxo Species in Catalytic Oxidations* (Ed.: B. Meunier), Springer, Berlin, **2000**.
[2] For an early review about metallocorrole complexes, see: C. Erlen, S. Will, K. M. Kadish, in *Porphyrin Handbook*, *Vol. 2* (Eds.: K. M. Kadish, K. M. Smith, R. Guilard), Academic Press, New York, **2000**, pp. 233–300.
[3] Z. Gross, N. Galili, I. Saltsman, *Angew. Chem.* **1999**, *111*, 1530–1533; *Angew. Chem. Int. Ed.* **1999**, *38*, 1427–1429.
[4] Z. Gross, H. B. Gray, *Adv. Synth. Catal.* **2004**, *346*, 165–170, and references therein.
[5] Z. Gross, G. Golubkov, L. Simkhovich, *Angew. Chem.* **2000**, *112*, 4211–4213; *Angew. Chem. Int. Ed.* **2000**, *39*, 4045–4047.
[6] A. Mahammed, Z. Gross, *J. Am. Chem. Soc.* **2005**, *127*, 2883–2887.
[7] G. Golubkov, J. Bendix, H. B. Gray, A. Mahammed, I. Goldberg, A. J. DiBilio, Z. Gross, *Angew. Chem.* **2001**, *113*, 2190–2192; *Angew. Chem. Int. Ed.* **2001**, *40*, 2132–2134.
[8] H. Y. Liu, T. S. Lai, L. L. Yeung, C. K. Chang, *Org. Lett.* **2003**, *5*, 617–620.
[9] B. S. Mandimutsira, B. Ramdhanie, R. C. Todd, H. L. Wang, A. A. Zareba, R. S. Czernuszewicz, D. P. Goldberg, *J. Am. Chem. Soc.* **2002**, *124*, 15170–15171.
[10] R. Zhang, M. Newcomb, *J. Am. Chem. Soc.* **2003**, *125*, 12418–12419.
[11] R. Zhang, J. H. Horner, M. Newcomb, *J. Am. Chem. Soc.* **2005**, *127*, 6573–6582.
[12] R. Zhang, R. E. P. Chandrasena, E. Martinez II, J. H. Horner, M. Newcomb, *Org. Lett.* **2005**, *7*, 1193–1195.
[13] R. Paolesse, S. Nardis, F. Sagone, R. G. Khoury, *J. Org. Chem.* **2001**, *66*, 550–556.
[14] D. T. Gryko, B. Koszarna, *Synthesis* **2004**, 2205–2209, and references therein.
[15] E. Steene, T. Wondimagegn, A. Ghosh, *J. Phys. Chem. B* **2001**, *105*, 11406–11413.
[16] A. D. Alder, F. R. Longo, F. Kampas, J. Kim, *J. Inorg. Nucl. Chem.* **1970**, *32*, 2443–2445.
[17] M. Hoshino, S. Arai, M. Yamaji, Y. Hama, *J. Phys. Chem.* **1986**, *90*, 2109–2111.
[18] J. P. Collman, L. Zeng, R. A. Decréau, *Chem. Commun.* **2003**, 2974–2975.
[19] K. S. Suslick, R. A. Watson, *New J. Chem.* **1992**, *16*, 633–642; H. Hennig, *Coord. Chem. Rev.* **1999**, *182*, 101–123.
[20] J. T. Groves, J. Lee, S. S. Marla, *J. Am. Chem. Soc.* **1997**, *119*, 6269–6273.
[21] N. Jin, J. T. Groves, *J. Am. Chem. Soc.* **1999**, *121*, 2923–2924.
[22] W. Nam, I. Kim, M. H. Lim, H. J. Choi, J. S. Lee, H. G. Jang, *Chem. Eur. J.* **2002**, *8*, 2067–2071.
[23] G. Golubkov, Z. Gross, *J. Am. Chem. Soc.* **2005**, *127*, 3258–3259.
[24] P. E. Ellis, J. W. Lyons, *Coord. Chem. Rev.* **1990**, *105*, 181–193.
[25] M. W. Grinstaff, M. G. Hill, J. A. Labinger, H. B. Gray, *Science* **1994**, *264*, 1311–1313.
[26] D. Dolphin, T. G. Traylor, L. Y. Xie, *Acc. Chem. Res.* **1997**, *30*, 251–259.
[27] S. H. Wang, B. S. Mandimutsira, R. Todd, B. Ramdhanie, J. P. Fox, D. P. Goldberg, *J. Am. Chem. Soc.* **2004**, *126*, 18–19.

Received: February 8, 2005
Revised: May 8, 2005
Published online: July 20, 2005

